Published in : Epilepsia. 2019;60:2325-2333.
DOI: DOI: 10.1111/epi.16353
Status : Postprint (Author's version)

EX VIVO CHARACTERIZATION OF NEUROINFLAMMATORY AND NEURORECEPTOR CHANGES DURING EPILEPTOGENESIS USING CANDIDATE POSITRON EMISSION TOMOGRAPHY BIOMARKER

Pablo Bascunana[1] | Thibault Gendron[2,3] | Kerstin Sander[2,3] | Ina Jahreis[1,4] |Andras Polyak[1] | Tobias L. Ross[1] | Marion Bankstahl[4,5] | Erik Arstad[2,3] |Jens P. Bankstahl[1]

[1]*Department of Nuclear Medicine, Hannover Medical School, Hannover, Germany*
[2]*Institute of Nuclear Medicine, University College London, London, UK*
[3]*Department of Chemistry, University College London, London, UK*
[4]*Department of Pharmacology, Toxicology and Pharmacy, University of Veterinary Medicine, Hannover, Germany*
[5]*Institute for Laboratory Animal Science, Hannover Medical School, Hannover, Germany*

Authors Bascunana and Gendron contributed equally to this study.

Pablo Bascunana https://orcid.org/0000-0003-2186-8899 Jens P. Bankstahl https://orcid.org/0000-0003-4735-4490

ABSTRACT

Objective: Identification of patients at risk of developing epilepsy before the first spontaneous seizure may promote the development of preventive treatment providing opportunity to stop or slow down the disease.

Methods: As development of novel radiotracers and on-site setup of existing radiotracers is highly time-consuming and expensive, we used dual-centre in vitro autoradiography as an approach to characterize the potential of innovative radiotracers in the context of epilepsy development. Using brain slices from the same group of rats, we aimed to characterise the evolution of neuroinflammation and expression of inhibitory and excitatory neuroreceptors during epileptogenesis using translational positron emission tomography (PET) tracers; ^{18}F-flumazenil (^{18}F-FMZ; $GABA_A$ receptor), ^{18}F-FPEB (metabotropic glutamate receptor 5; mGluR5), ^{18}F-Autriciclamide (translocator protein; TSPO, microglia activation) and ^{18}F-deprenyl (monoamine oxidase B, astroglia activation). Autoradiography images from selected time points after pilocarpine-induced status epilepticus (SE; baseline, 24 and 48 hours, 5, 10 and 15 days and 6 and 12-14 weeks after SE) were normalized to a calibration curve, co-registered to an MRI-based 2D region-of-interest atlas, and activity concentration (Bq/mm^2) was calculated.

Results: In epileptogenesis-associated brain regions, ^{18}F-FMZ and ^{18}F-FPEB showed an early decrease after SE. ^{18}F-FMZ decrease was maintained in the latent phase and further reduced in the chronic epileptic animals, while ^{18}F-FPEB signal recovered from day 10, reaching baseline levels in chronic epilepsy. ^{18}F-Autriciclamide

Published in : Epilepsia. 2019;60:2325-2333.
DOI: DOI: 10.1111/epi.16353
Status : Postprint (Author's version)

showed an increase of activated microglia at 24 hours after SE, peaking at 5-15 days and decreasing during the chronic phase. On the other hand, ^{18}F-deprenyl autoradiography showed late astrogliosis, peaking in the chronic phase.

Significance: Autoradiography revealed different evolution of the selected targets during epileptogenesis. Our results suggest an advantage of combined imaging of inter-related targets like glutamate and GABAa receptors, or microglia and astrocyte activation, in order to identify important interactions, especially when using PET imaging for the evaluation of novel treatments.

KEYWORDS
astroglia, epilepsy, GABAA receptor, glutamate receptor, microglia

KEY POINTS

- In vitro autoradiography may assist identifying imaging biomarkers for epileptogenesis
- $GABA_A$ receptor and mGluR5 density decreases after SE, only partially recovering for mGluR5 during late epileptogenesis
- Epileptogenesis is accompanied by early microglial activation while astrocytosis may be linked to the occurrence of seizures
- Combining of imaging biomarkers for inter-related targets may provide critical understanding in the study of epileptogenesis

Published in : Epilepsia. 2019;60:2325-2333.
DOI: DOI: 10.1111/epi.16353
Status : Postprint (Author's version)

INTRODUCTION

Epilepsy is one of the most common neurological diseases and affects about 60 million people worldwide.[1] Epileptogenesis, the process that transforms a healthy brain into a brain suffering seizures, involves several different processes such as neuroinflammation, metabolic and neurotransmitter and/or receptor alterations, or blood brain barrier impairment.[2] In addition, 30-40% of the patients suffer from refractory epi- 3 lepsy, ie epilepsy that cannot be controlled by medication.[3] Currently, epilepsy treatments are mainly symptomatic treatments that supress recurrent seizures. However, identification of antiepileptogenic treatments might slow down the disease progression or even prevent epilepsy. Still, this strategy requires the identification of subjects susceptible of developing epilepsy, ie with active epileptogenesis. Thus, there is a need for identifying epileptogenesis biomarkers to select the target population of antiepileptogenic treatments.

Positron emission tomography (PET) has been widely used for pre-surgical location of epileptic foci in epilepsy patients with non-conclusive magnetic resonance images (MRI). Traditionally, 2-fluorodeoxyglucose (^{18}F-FDG) is the tracer of choice for this aim.[4,5] An asymmetric glucose hypometabolism may indicate the location of the epileptic focus. However, not all the patients show this asymmetry and in recent years, other radiotracers have been investigated as tools to localise the epileptic focus, showing sometimes even higher sensitivity than ^{18}F-FDG. Investigational tracers bind to neuroreceptors as gamma-aminobutyric acid (GABA) receptor, serotonin receptors or targets associated with neuroin- flammation,[6,7] as the imbalance between glutamatergic and gabaergic neurotransmission as well as neuroinflammation 8 are considered to play a key role in epileptogenesis.[8]

However, the knowledge about alterations on these imaging targets during epileptogenesis is limited as epilepto- genesis is very difficult to be studied in human patients as no biomarker exits to identify patients in risk of developing epilepsy. Thus, animal models are used to study alterations during epileptogenesis. Among epileptogenesis animal models, the rat pilocarpine model is one of the most investigated.[9] This model is characterized by recurrent epileptic seizures after a latent phase following an induced *status epilepticus* (SE). Development of spontaneous recurrent seizures is achieved in almost all animals when the SE duration is 90 minutes or more making this model suitable for investigations of early epileptogenesis-associated changes in brain tissue.[10] Neuroinflammation and neuronal loss among other alterations have been described in this model[11-13] as well as comorbidities also seen in patients such as anxiety and cognitive impairment.[14] In addition, imaging studies have shown down-regulation of $GABA_A$ receptors after the epileptogenic insult[15-17] and decrease of metabotropic glutamate receptor 5 (mGluR5) in the acute and subacute phases after SE recovering baseline levels in the chronic phase.[18] In addition, we and others have previously described microglial activation time profile in different animal models of epileptogenesis showing a rapid activation of microglial cells peaking in the first weeks after the insult.[13,19-22]

The aim of this study was to characterise binding of four PET imaging tracers in the acute, latent and chronic phase of epileptogenesis in the rat pilocarpine post SE rat model, and to determine their potential as epileptogenesis biomarkers, either as single tracers and/or in combination. We used quantitative phosphor imaging to be able to (i) compare a range of radiotracers depicting different biological targets within the same

Published in : Epilepsia. 2019;60:2325-2333.
DOI: DOI: 10.1111/epi.16353
Status : Postprint (Author's version)

group of animals, and (ii) to quantify tracer uptake in selected brain area relevant to epileptogenesis. Thus, series of brain slices from the same animals were incubated with different radiotracers targeting the $GABA_A$ receptor (N-(1-(3-[^{18}F]fluorophenyl)propan-2-yl)-N-meth- ylprop-2-yn-1-amine (^{18}F-FMZ)), and mGluR5 (3-[^{18}F]flu- oro-5-(pyridin-2-ylethynyl)benzonitrile (^{18}F-FPEB)), as well as the translocator protein (TSPO; ^{18}F-flutriciclamide, also known as ^{18}F-GE180) and monoamine oxidase B (MAO-B; ethyl 8-[^{18}F]fluoro-5-methyl-6-oxo-*4H*-imidazo[1,5-a][1,4] benzodiazepine-3-carboxylate (^{18}F-deprenyl)) as neuroinflammation markers (microglial and astroglial activation, respectively).

MATERIAL AND METHODS

ANIMALS

Female Sprague-Dawley rats (n = 33; 200-220 g at the start of experiments; Envigo, Italy) were housed in pairs in individually ventilated bio-containment units under a 14/10-hour light/dark cycle. Standard laboratory chow (Altromin 1324) and autoclaved tap water were freely accessible at every time. Animals were allowed to adapt to housing conditions and repetitive handling for at least 1 week before starting the experiments. All the experiments were conducted in accordance with European Communities Council Directive 2010/63/EU and were formally approved by the responsible local authority (Niedersachsisches Landesamt für Verbraucherschutz und Lebensmittelsicherheit). Data are reported in accordance with the ARRIVE guidelines.

Status epilepticus induction

SE was induced as described previously.[23] Briefly, rats (n = 45) were pre-treated with lithium chloride (127 mg/kg, p.o.) 14-16 hours before pilocarpine administration. Methyl-scopolamine (1 mg/kg, i.p.) was administered 30 minutes prior to an i.p. bolus of 30 mg/kg pilocarpine hydrochloride, followed by a maximum of 3 injections of 10 mg/kg i.p. at 30 minutes intervals as needed until SE onset, defined by sustained convulsive seizures (score 4 and 5 according to Racine's scale[24]). SE was interrupted after 90 minutes by administration of diazepam (10 mg/kg, i.p.; Ratiopharm). If needed, diazepam injection was repeated up to two times (2nd repetition 5 mg/kg) at 15 minutes intervals. Following SE, rats were hand-fed with mashed laboratory chow and received injections of glucose electrolyte solution (Sterofundin® HEG-5; Braun) until recovery. SE success rate was 93% (38/41) after injecting an average pilocarpine dose of 36.5 ± 7.5 mg/kg. Animals which did not exhibit SE were excluded from further experiments. The post-SE mortality rate was 24% (9/38) within the first 48 hours. Seizures observed whenever a trained investigator was in the animal room were documented. No continuous monitoring was performed, but all animals of the chronic epilepsy group exhibited at least two generalized spontaneous seizures before euthanasia and were therefore classified as chronic epileptic.

Animals were euthanized at various time points: baseline (ie naïve animals; n = 4) and 24 hours (n = 4), 48 hours (n = 4), 5 days (n = 4), 10 days (n = 4), 15 days (n = 4) and 6 weeks (n = 4) after SE, and in the chronic epilepsy phase (12-14 weeks after SE; n = 5). Animals were decapitated under anaesthesia and brains were removed and snap frozen in 2-methylbutane (Sigma-Aldrich) immersed in liquid nitrogen. The brains were sliced in a

Published in : Epilepsia. 2019;60:2325-2333.
DOI: DOI: 10.1111/epi.16353
Status : Postprint (Author's version)

cryostat (Shandon) with a slice thickness of 14 µm at three different section levels relative to bregma: 0.0, -3.6, and -5.2 mm. Slides were stored and shipped frozen at -20°C until the autoradiography was performed.

RADIOCHEMISTRY

The radiosynthesis of ^{18}F-flutriciclamide was carried out at Hannover Medical School as previously described.[19] ^{18}F-flu- triciclamide was obtained in 18 ± 8% (n ≥ 20) decay-corrected radiochemical yield (d.c. RCY), the radiochemical purity was ≥ 99% and the molar activity of the radiotracer was 310-470 GBq/µmol. ^{18}F-Autriciclamide was formulated in an aqueous saline solution of 0.9% (containing 10-15% ethanol) prior to use for autoradiography experiments.

The radiosyntheses of ^{18}F-FMZ was carried out at Hannover Medical School following previously reported methods adapted to an automated synthesis module.[25,26] N.c.a. ^{18}F-fluoride was produced using the ^{18}O(p,n)^{18}F nuclear reaction at a Scanditronix MC35 cyclotron. The ^{18}F-la- beling of ^{18}F-FMZ was performed using the corresponding nitromazenil precursor (12 mg) in *N,N*-dimethylformamide (1.0 ml) and a potassium carbonate (1.6 mg) Kryptofix[2.2.2] (10.0 mg) system. The radiosynthesis was automated on a self-designed radiosynthesis apparatus in a custom-made cassette system. The crude labeling mixture was purified on a RP (C18) semi-prep HPLC system using an isocratic eluent of 0.05 mol/L sodium actetate buffer/tetrahydrofuran/ methanol (80:10:10) at 3 mL/min flow. The product fraction was isolated and formulated in 0.9% saline (10-15% ethanol) after SPE(C18)-based solvent change. ^{18}F-FMZ was obtained in 8 ± 4% (n ≥ 10) d.c. RCY, the radiochemical purity was ≥ 96% and the molar activity of the radiotracer was 35-84 GBq/µmol.

The radiosyntheses of ^{18}F-FPEB and 3-^{18}F-fluorodepre- nyl were carried out at the University College London as previously reported.[27] [^{18}F]FPEB was obtained in 55 ± 3 (n = 12) d.c. RCY with a radiochemical purity > 98% and a molar activity of 13-20 GBq/µmol. 3-^{18}F-fluorodeprenyl was obtained in 32 ± 2% (n = 3) d.c. RCY, the radiochemical purity was >98% and the molar activity of the tracer was 17-30 GBq/µmol. Both radiotracers were formulated in an aqueous solution of sodium phosphate buffer (21 mmol/L, 5 mL, containing 10% ethanol) prior to use for autoradiography experiments.

AUTORADIOGRAPHY

Quantitative phosphor imaging autoradiography was performed at both sites using protocols optimized for each tracer. All tissue samples were incubated together for each tracer to avoid potential differences between repeated tracer syntheses. Experiments with FMZ and GE-180 were carried out as described before.[13] Briefly, brain sections were pre-incubated for 30 minutes at room temperature in 50 mmol/L phosphate buffer saline (PBS; pH 7.4), followed by incubation with the target tracer for 30 minutes. After incubation, slides were washed with ice-cold PBS and rinsed in distilled water to remove buffer salts. Once dried, slides were placed in a cassette and exposed to a high-resolution phosphor imaging plate (PerkinElmer/GE Healthcare) for 30 minutes. FPEB was formulated in Tris-buffered saline (TBS; pH 7.4) and 3-^{18}F- fluorodeprenyl in PBS. Pre-washed (TBS; 30 minutes or PBS; 20 minutes) tissue sections were incubated with tracer solution for a duration of 2 or 1 hours, respectively. Slides were washed three times in ice-cold PBS and subsequently dipped in water. After drying, tissue sections were exposed overnight to a high-resolution storage phosphor screen (GE

Published in : Epilepsia. 2019;60:2325-2333.
DOI: DOI: 10.1111/epi.16353
Status : Postprint (Author's version)

Healthcare).

All brain tissue sections were exposed together with standardised samples, which were used to obtain a calibration curve for each experiment. The calibration curves were obtained by including a dilution series with known activity concentrations. After exposure, the phosphor-plate was then digitalized in a phosphor imaging scanner (Cyclone, PerkinElmer/Typhoon, GE Healthcare).

Data analysis was performed at a single site by an expert blinded to the animal groups investigated using Pmod 3.7 (Pmod software, Pmod Technologies, Zurich, Switzerland). First, signal intensity of the calibration curve was determined and the calibration factor calculated with a regression analysis as previously described.[13] A 3D regions-of-interest (ROI) atlas drawn on an MRI template[28] was converted to 2D and, then, the autoradiography films were co-registered to the corresponding 2D ROI slice. ROIs were manually adapted if slice quality was not optimal. Activity concentration (Bq/ mm^2) in hippocampus, piriform cortex, amygdala, and thalamus was calculated.

STATISTICS

Data were analyzed using statistical software (Graphpad Prism 7, La Jolla, CA, USA). Group sizes were guided by power analysis before starting the experiments. Differences between time points were analysed by ANOVA followed by Dunnett's post hoc test with baseline as control group. Differences were considered statistically significant when $P < .05$. Data are shown as mean ± standard deviation (SD).

RESULTS

Autoradiography with ^{18}F-FMZ targeting the $GABA_A$ receptor showed an initial generalized decrease after SE being statistically significant already at 24 hours in amygdala and piriform cortex (-28%, $P = .032$ and -43%, $P = .005$, respectively), with a partial recovery at 5 days post-SE (Figure 1A,B). After decreasing again from 15 days onwards, the ^{18}F-FMZ signal was further reduced in the chronic phase in amygdala and piriform cortex (-49%, $P < .001$ and -51%, $P = .002$, respectively), as well as in the hippocampus (-41%; $P = .007$). Although the curve shape was similar for thalamus no statistically significant differences in ^{18}F-FMZ signal were detected.

^{18}F-FPEB binding, which reflects the levels of mGluR5 expression, decreased at 24 hours after SE in hippocampus and thalamus (-15%, $P = .006$ and -18%, $P = .003$, respectively; Figure 1C,D). This decrease was maintained until 10 days after SE. At 15 days post SE, only hippocampus showed significant differences to baseline levels (-15%, $P = .004$). In the chronic phase, 6 and 12 weeks after SE, none of the regions investigated differed significantly from the control animals.

In addition, as an imbalance between inhibition and excitation is theorized to happen during epileptogenesis, we evaluated the evolution of the ratio between glutamatergic and GABAergic systems represented by ^{18}F-FMZ and ^{18}F-FPEB autoradiography during epileptogenesis (Figure 1E). Both tracers showed a reduction during the acute phase being more pronounced in the GABAergic system at 24 and 48 hours after SE. The ratio between glutamatergic (mGluR5) and GABAergic receptor populations recovered during the latent phase until 15 days

Published in : Epilepsia. 2019;60:2325-2333.
DOI: DOI: 10.1111/epi.16353
Status : Postprint (Author's version)

after SE, when the partial recovery of ^{18}F-FPEB signal and the maintained reduction in ^{18}F-FMZ resulted in an imbalance between GABA and glutamate receptors. This imbalance became again evident at the chronic epileptic phase.

^{18}F-Flutriciclamide targeting TSPO, as a marker of activated microglia, showed a global increase of binding at 24 hours post SE, increasing during the latent phase in all investigated regions (Figure 2A,B). Amygdala and thalamus TSPO signal peaked at 5 days post SE (+370%, $P < .001$ and +437%, $P < .001$, respectively) while piriform cortex maximum binding was at 10 days post SE (+505%, $P < .001$) and hippocampus at 15 days after SE (+247%, $P < .001$). Compared to the peak values, TSPO signal decreased towards the chronic phase of epileptogenesis, ie 6 and 12 weeks post SE, in all the regions analysed but not reaching baseline levels.

Following a non-significant decrease shortly after SE, 18

^{18}F-deprenyl autoradiography revealed significant MAO-B upregulation in the late latent phase (15 days post SE) in the hippocampus (+54%, $P = .001$; Figure 2C,D). In chronic epilepsy, upregulation was present in all the regions studied (eg hippocampus: +102%, $P < .001$).

FIGURE 1 A, Representative ^{18}F-FMZ autoradiography coronal slices for each experimental time point in cold scale and B, group quantification shown as bar graph. C, Representative ^{18}F-FPEB autoradiography slices for each experimental time point and D, quantified signal (Bq/ mm^2) for at each time point. E, Intensity ratio between ^{18}F-FMZ and ^{18}F-FPEB binding in each individual animal. Data are shown as mean ± SD of 4-5 animals per time point. Color-coded asterisks for each region indicate significant changes ($P < .05$) compared to the control group (baseline)

Published in : Epilepsia. 2019;60:2325-2333.
DOI: DOI: 10.1111/epi.16353
Status : Postprint (Author's version)

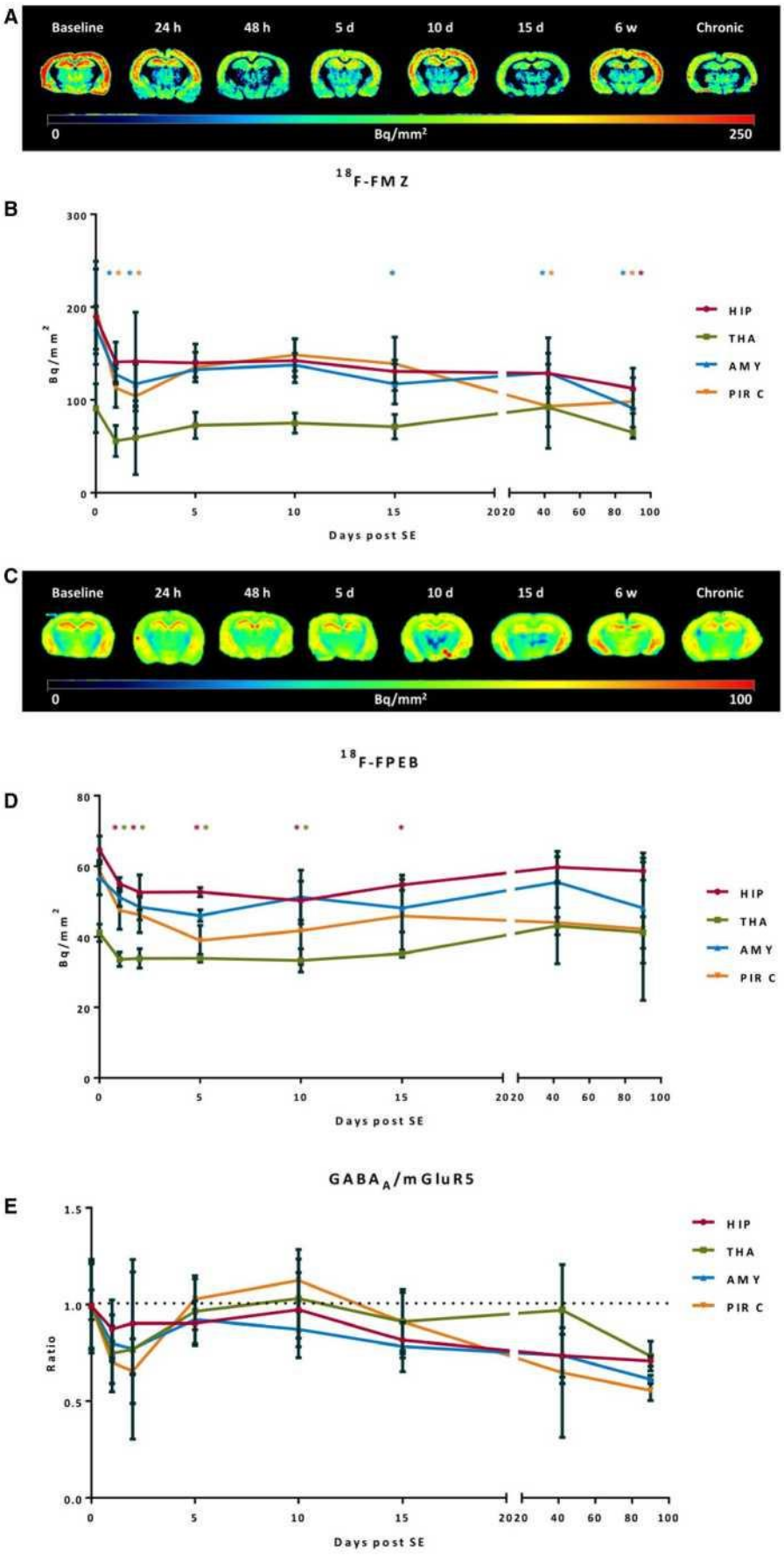

Published in : Epilepsia. 2019;60:2325-2333.
DOI: DOI: 10.1111/epi.16353
Status : Postprint (Author's version)

FIGURE 2 A, Representative ^{18}F-flutriciclamide autoradiography coronal slices for each experimental time point in cold scale and B, group quantification shown as bar graph. C, Representative ^{18}F-deprenyl autoradiography slices for each experimental time point. D, Graph showing group quantification at each time point. Data are shown as mean ± SD of 4-5 animals per time point. Color-coded asterisks for each region indicate significant changes ($P < .05$) compared to the control group (baseline)

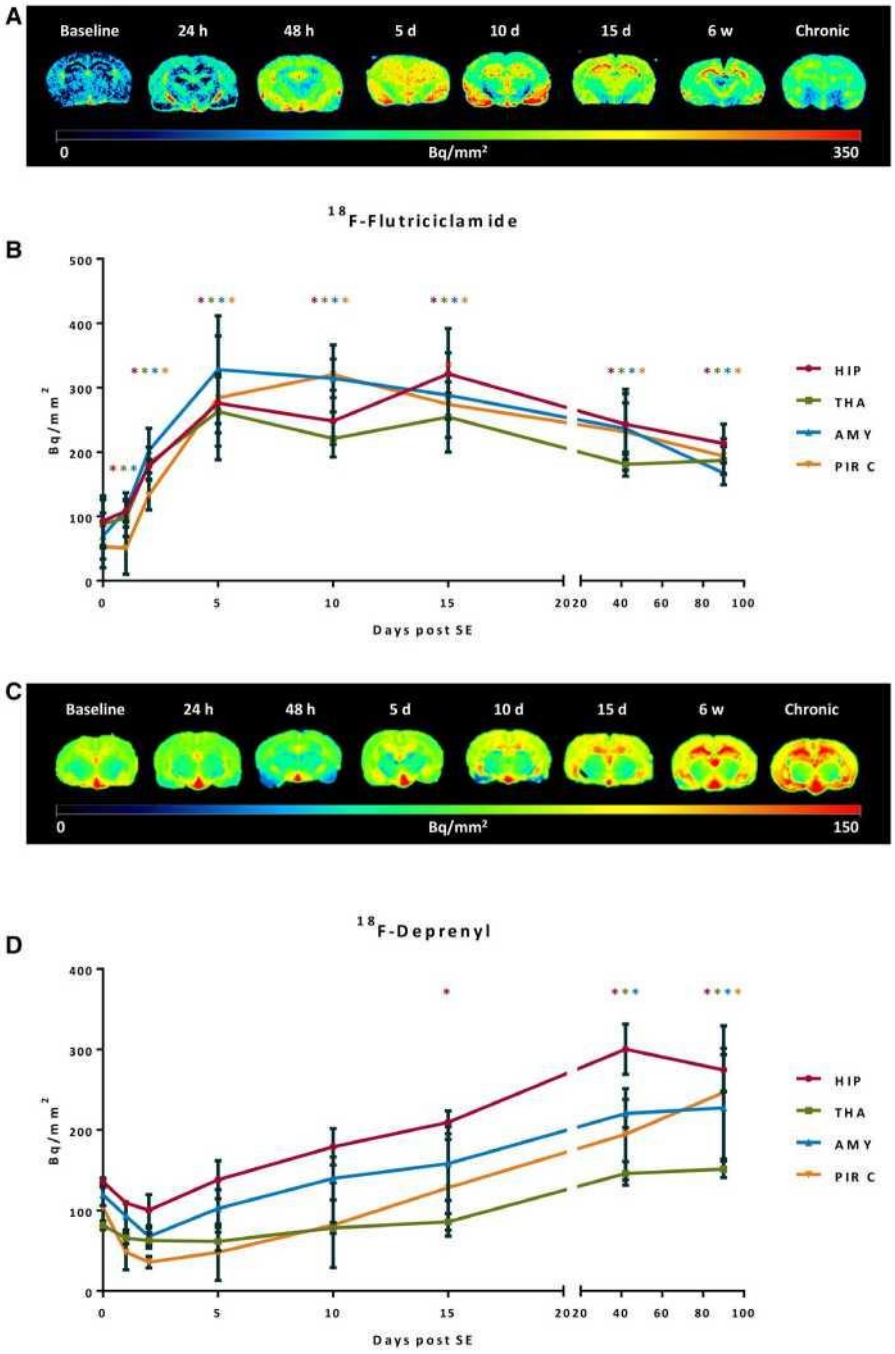

Published in : Epilepsia. 2019;60:2325-2333.
DOI: DOI: 10.1111/epi.16353
Status : Postprint (Author's version)

DISCUSSION

With the aim of assessing the suitability of four PET tracers depicting different biological targets to depict epileptogenesis in vivo, we have carried out a longitudinal autoradiography study to assess tracer binding in a rat model of epilepsy. Imaging biomarkers are of great interest as they enable
several in vivo measurement in a minimally invasive manner and allow visualization of molecular pathways involved in epileptogenesis.[29,30] Here, we describe the evolution of tracer binding to mGluR5, $GABA_A$ receptors, and microglia and astroglia markers during epileptogenesis and chronic epilepsy in the lithium-pilocarpine post-SE model in rats. The use of in vitro autoradiography enabled direct quantification and comparison of all tracers in brain slices from the same animals for each time point. All four targets have shown alterations during epileptogenesis with apparently different time profiles.

Choi et al have previously described alterations in mGluR5 after pilocarpine-induced SE by in vivo PET imaging.[18] They reported a global decrease of mGluR5 expression in the acute phase after SE that was maintained in hippocampus and amygdala in the subacute and chronic phases. In our experiments with FPEB, we confirmed the reduced tracer binding during the acute phase after SE. During the latent phase of epileptogenesis tracer binding was found to be comparable to that in healthy controls in most brain regions. Differences between in vivo and in vitro procedures (eg no radiotracer metabolism), as well as the use of different radiotracers to image mGluR5, may explain the divergent results in these studies as endogenous glutamate concentration may also play a role in in vivo mGluR5 binding.

^{18}F-FMZ autoradiography showed down-regulation of the benzodiazepine receptor already 24 hours after SE. Contrarily to what was observed with mGluR5 receptors, this reduction of tracer binding did not recover in the latent phase of epileptogenesis, and actually increased in the chronic phase. This suggests a decrease of GABAergic neurotransmission acutely as a consequence of the SE that does not recover afterwards during epileptogenesis. In addition, NeuN or Nissl staining in the same animal model has shown significant neuronal loss also already at 48 hours.[13,31] GABAergic neurons may be more sensitive to the brain insult,[32] which would explain the lack of recovery observed compared to the glutamatergic system.

Furthermore, we compared the ratio of tracer binding between glutamatergic and GABAergic neuroreceptor during epileptogenesis. An imbalance starting 15 days after SE was detected, driven by the recovery of mGluR5 signal while ^{18}F-FMZ remained subdued, or even further reduced at this time point. Interestingly, the imbalance was first detected at the end of the latent phase, approximately at the time when the first spontaneous seizures are usually present in this model.[33,34] The imbalance increased during epileptogenesis reaching maximum values in the chronic phase when the spontaneous seizures are more frequent. This finding may be related to the neuronal hyperexcitability described in epileptogenesis animal models, including the pilocarpine rat model, and could be a potential therapeutic antiepileptogenic target. In addition, imaging of both neurotransmitter systems may provide important additional information about epileptogenesis as changes in only one of the neurotransmitters does not provide information about the excitatory/inhibitory balance of the system.

TSPO expression has previously been investigated in this[11,13] and other animal models of epileptogenesis,[19-22,3]

Published in : Epilepsia. 2019;60:2325-2333.
DOI: DOI: 10.1111/epi.16353
Status : Postprint (Author's version)

and is known to be upregulated during epileptogenesis as shown by immunohistological staining of activated microglia.[13,21,22] Our in vitro data showed increased TSPO expression 24 hours after pilocarpine-induced SE, and that the peak expression occurs at different time points across the brain.

After an initial more generalized TSPO activation, epilepsy- related areas such as hippocampus, amygdala or piriform cortex showed maintained up-regulation during the latent phase (Figure 2A). Generalized TSPO activation may be directly induced by the initial insult, while the sustained activation in specific regions suggests that microglial activation may have a role in epileptogenesis, as often proposed.[36,37]

As part of the neuroinflammatory response, astrogliosis has been widely studied in epilepsy, including PET studies in epileptic patients.[38,39] However, to our knowledge, no PET studies targeting astrocytical activation in animal models of epileptogenesis have been published yet. Here, we tested a novel PET tracer, ^{18}F-deprenyl, targeting MAO-B as a marker of astrocyte activation.[27] In vitro autoradiography with this tracer showed a late response of astrocytes compared to the TSPO up-regulation seen with ^{18}F-flutriciclamide. MAO-B autoradiography showed no alterations during the acute phase after the epileptogenic insult, but a progressive increase during the latent phase, peaking at the chronic stage. The results suggest that astrocytes activation may be triggered by seizures. This time profile is consistent with the increased GFAP staining after pilocarpine-induced SE in rats[12,13] or after intrahippocampal kainate-induced SE in mice,[22] and confirms that ^{18}F-deprenyl binding reflects astrocyte activation. Nevertheless, the increase in MAO-B binding seems to be slightly delayed as compared to GFAP expression.

It is generally accepted that TSPO expression reflects reactive microglia, but some studies have suggested a significant contribution of reactive astrocytes.[22,40] However, in our study TSPO expression does not reflect the astroglial activation as determined by ^{18}F-deprenyl autoradiography. The late activation of astrocytes and the early TSPO peak seen in this study suggests that TSPO brain imaging mainly reflects microglial activation and not astrogliosis. These results contradict previous studies in a mouse model of SE, where late astrogliosis was paralleled by an increase of TSPO tracer up- take,[22] but are consistent with previous findings from rodent models of neuroinflammation in Alzheimer's disease[41] and myocardial infarction.[42] It is possible that the discrepancies reflect differences between species and neuroinflammation responses in these models.

Despite the advantage of in vitro evaluation of PET tracer candidates for identifying epileptogenesis biomarkers, this approach also has some limitations. We have only used the baseline group as control group, ie rats that were euthanized at an age corresponding to that of the animals euthanized during the acute phase of epileptogenesis. The lack of age-matched controls for the chronic epileptic animals as well as the use of only female rats may partially influence the translatability of our results. In the used animal model, first seizures occur 6-10 days after SE,[43] meaning that a truly seizure-free latent period is difficult to be investigated in this model. Nevertheless, it has to be considered that epileptogenesis does not stop after the first seizure and molecular changes will evolve in a continuum. Differences between in vitro autoradiography and in vivo PET imaging, in particular the absence of perfusion, have to be considered. In addition, PET tracers are often metabolised after injection, in contrast to in vitro autoradiography. Therefore, tracer binding studies with in vitro autoradiography cannot always directly be interpolated with in vivo PET. However, the focus of this study was on changes in the tracer binding distribution of these targets aiming to select candidates for

Published in : Epilepsia. 2019;60:2325-2333.
DOI: DOI: 10.1111/epi.16353
Status : Postprint (Author's version)

further longitudinal prognostic biomarker studies in animal models in which only part of the animals become epileptic.[23] For these studies potential in vivo metabolism of the radiotracers needs also to be considered as this does not take place when using autoradiography. While we cannot securely conclude on the prognostic value of the biomarker candidates, we expect that the temporal interplay of the binding profile of the tracers investigated will help to guide the choice of tracers and the experimental design for future longitudinal PET studies.

Autoradiography here presented provides a time profile of neuroreceptor and neuroinflammation alterations during epi- Ieptogenesis in the rat-pilocarpine model. This temporal and target information will assist in the optimal choice for future PET studies in epileptogenesis and epilepsy. While its time profile suggests microglia activation as a biomarker for early epileptogenesis, astrocyte activation may be linked to the occurrence of seizures. In addition, divergent evolution of gabaergic and glutamatergic receptors after SE suggests that combination of inter-related targets may provide a promising strategy for epileptogenesis biomarkers and/or therapeutic targets.

ACKNOWLEDGEMENTS

This study was funded by the European Seventh's Framework Programme (FP7/2007-2013) under grant agreement n°602102 (EPITARGET). I. Jahreis was supported by a scholarship from the Konrad-Adenauer-Stiftung e.V. We thank GE Healthcare for providing the general method and access to the precursor for ^{18}F-flutriciclamide synthesis. K. Sander is funded by Mallinckrodt. This work was undertaken in part at UCLH/UCL, which is funded in part by the Department of Health's NIHR Biomedical Research Centres funding scheme.

CONFLICT OF INTEREST

None of the authors has any conflict of interest to disclose. We confirm that we have read the Journal's position on issues involved in ethical publication and affirm that this report is consistent with those guidelines.

REFERENCES

1. Baulac M, de Boer H, Elger C, Glynn M, Kalviainen R, Little A, et al. Epilepsy priorities in Europe: a report of the ILAE-IBE Epilepsy Advocacy Europe Task Force. Epilepsia. 2015;56:1687-95.
2. Pitkanen A, Lukasiuk K, Dudek FE, Staley KJ. Epileptogenesis. Cold Spring Harb Perspect Med. 2015;5:a022822.
3. Kobau R, Zahran H, Thurman DJ, Zack MM, Henry TR, Schachter SC, et al. Epilepsy surveillance among adults-19 states, behavioral risk factor surveillance system, 2005. MMWR Surveill Summ. 2008;57:1-20.
4. O'Brien TJ, Miles K, Ware R, Cook MJ, Binns DS, Hicks RJ. The cost-effective use of 18F-FDG PET in the presurgical evaluation of medically refractory focal epilepsy. J Nucl Med. 2008;49:931-7.
5. Willmann O, Wennberg R, May T, Woermann FG, Pohlmann-Eden B. The contribution of 18F-FDG PET in preoperative epilepsy surgery evaluation for patients with temporal lobe epilepsy a metaanalysis. Seizure. 2007;16:509-20.

Published in : Epilepsia. 2019;60:2325-2333.
DOI: DOI: 10.1111/epi.16353
Status : Postprint (Author's version)

6. Liew CJ, Lim YM, Bonwetsch R, Shamim S, Sato S, Reeves-Tyer P, et al. 18F-FCWAY and 18F-FDG PET in MRI-negative temporal lobe epilepsy. Epilepsia. 2009;50:234-9.
7. Vivash L, Gregoire M-C, Lau EW, Ware RE, Binns D, Roselt P, et al. 18F-flumazenil: a γ-aminobutyric acid A-specific PET radiotracer for the localization of drug-resistant temporal lobe epilepsy. J Nucl Med. 2013;54:1270-7.
8. Pitkanen A, Loscher W, Vezzani A, Becker AJ, Simonato M, Lukasiuk K, et al. Advances in the development of biomarkers for epilepsy. Lancet Neurol. 2016;15:843-56.
9. Martm E, Pozo M. Animal models for the development of new neuropharmacological therapeutics in the status epilepticus. Curr Neuropharmacol. 2006;4:33-40.
10. Cavalheiro EA, Leite JP, Bortolotto ZA, Turski WA, Ikonomidou C, Turski L. Long-term effects of pilocarpine in rats: structural damage of the brain triggers kindling and spontaneous recurrent seizures. Epilepsia. 1991;32:778-82.
11. Yankam Njiwa J, Costes N, Bouillot C, Bouvard S, Fieux S, Becker G, et al. Quantitative longitudinal imaging of activated microglia as a marker of inflammation in the pilocarpine rat model of epilepsy using [11C]-(R)-PK11195 PET and MRI. J Cereb Blood Flow Metab. 2016;37:1251-63.
12. Zhang L, Guo Y, Hu H, Wang J, Liu Z, Gao F. FDG-PET and NeuN-GFAP immunohistochemistry of hippocampus at different phases of the pilocarpine model of temporal lobe epilepsy. Int J Med Sci. 2015;12:288-94.
13. Brackhan M, Bascunana P, Postema JM, Ross TL, Bengel FM, Bankstahl M, et al. Serial quantitative TSPO-targeted PET reveals peak microglial activation up to 2 weeks after an epileptogenic brain insult. J Nucl Med. 2016;57:1302-8.
14. Lopes MW, Lopes SC, Santos DB, Costa AP, Gonçalves FM, de Mello N, et al. Time course evaluation of behavioral impairments in the pilocarpine model of epilepsy. Epilepsy Behav. 2016;55:92-100.
15. Morimoto K, Watanabe T, Ninomiya T, Hirao T, Tanaka A, Onishi T, et al. Quantitative evaluation of central-type benzodiazepine receptors with [(125)I]Iomazenil in experimental epi- leptogenesis: II. The rat cortical dysplasia model. Epilepsy Res. 2004;61:113-8.
16. Tamagami H, Morimoto K, Watanabe T, Ninomiya T, Hirao T, Tanaka A, et al. Quantitative evaluation of central-type benzodiazepine receptors with [(125)I] Iomazenil in experimental epileptogenesis. I. The rat kainate model of temporal lobe epilepsy. Epilepsy Res. 2004;61:105-12.
17. Vivash L, Gregoire M-C, Bouilleret V, Berard A, Wimberley C, Binns D, et al. In vivo measurement of hippocampal GABAA/ cBZR density with [18F]-flumazenil PET for the study of disease progression in an animal model of temporal lobe epilepsy. PLoS ONE. 2014;9:e86722.
18. Choi H, Kim YK, Oh SW, Im H-J, Hwang DW, Kang H, et al. In vivo imaging of mGluR5 changes during epileptogenesis using [11C]ABP688 PET in pilocarpine-induced epilepsy rat model. PLoS ONE. 2014;9:e92765.
19. Brackhan M, Bascunana P, Ross TL, Bengel FM, Bankstahl JP, Bankstahl M. [(18) F]GE180 positron emission tomographic imaging indicates a potential double-hit insult in the intrahippocampal kainate mouse model of temporal lobe epilepsy. Epilepsia. 2018;59:617-26.
20. Amhaoul H, Staelens S, Dedeurwaerdere S. Imaging brain inflammation in epilepsy. Neuroscience.

Published in : Epilepsia. 2019;60:2325-2333.
DOI: DOI: 10.1111/epi.16353
Status : Postprint (Author's version)

2014;279:238-52.

21. Dedeurwaerdere S, Callaghan PD, Pham T, Rahardjo GL, Amhaoul H, Berghofer P, et al. PET imaging of brain inflammation during early epileptogenesis in a rat model of temporal lobe epilepsy. EJNMMI Res. 2012;2:60.

22. Nguyen DL, Wimberley C, Truillet C, Jego B, Caillé F, Pottier G, et al. Longitudinal positron emission tomography imaging of glial cell activation in a mouse model of mesial temporal lobe epilepsy: toward identification of optimal treatment windows. Epilepsia. 2018;59:1234-44.

23. Brandt C, Toellner K, Klee R, Broer S, Loscher W. Effective termination of status epilepticus by rational polypharmacy in the lithium-pilo- carpine model in rats: window of opportunity to prevent epilepsy and prediction of epilepsy by biomarkers. Neurobiol Dis. 2015;75:78-90.

24. Racine RJ. Modification of seizure activity by electrical stimulation. II. Motor seizure. Electroencephalogr Clin Neurophysiol. 1972;32:281-94.

25. Massaweh G, Schirrmacher E, la Fougere C, Kovacevic M, Wangler C, Jolly D, et al. Improved work-up procedure for the production of [(18)F]flumazenil and first results of its use with a high- resolution research tomograph in human stroke. Nucl Med Biol. 2009;36:721-7.

26. Ryzhikov NN, Seneca N, Krasikova RN, Gomzina NA, Shchukin E, Fedorova OS, et al. Preparation of highly specific radioactivity [18F]flumazenil and its evaluation in cynomolgus monkey by positron emission tomography. Nucl Med Biol. 2005;32:109-16.

27. Gendron T, Sander K, Cybulska K, Benhamou L, Sin PKB, Khan A, et al. Ring-closing synthesis of dibenzothiophene sulfonium salts and their use as leaving groups for aromatic (18)F-fluorina- tion. J Am Chem Soc. 2018;140:11125-32.

28. Schiffer WK, Mirrione MM, Biegon A, Alexoff DL, Patel V, Dewey SL. Serial microPET measures of the metabolic reaction to a microdialysis probe implant. J Neurosci Methods. 2006;155:272-84.

29. Koepp MJ, Arstad E, Bankstahl JP, Dedeurwaerdere S, Friedman A, Potschka H, et al. Neuroinflammation imaging markers for epi- leptogenesis. Epilepsia. 2017;58(Suppl 3):11-9.

30. van Vliet EA, Dedeurwaerdere S, Cole AJ, Friedman A, Koepp MJ, Potschka H, et al. WONOEP appraisal: imaging biomarkers in epilepsy. Epilepsia. 2017;58:315-30.

31. Bankstahl M, Breuer H, Leiter I, Markel M, Bascunana P, Michalski D, et al. Blood-brain barrier leakage during early epileptogenesis is associated with rapid remodeling of the neurovascular unit. eNeuro. 2018;5. https://doi.org/10.1523/ENEURO.0123-18.2018

32. Guerriero RM, Giza CC, Rotenberg A. Glutamate and GABA imbalance following traumatic brain injury. Curr Neurol Neurosci Rep. 2015;15:27.

33. Curia G, Longo D, Biagini G, Jones RS, Avoli M. The pilocarpine model of temporal lobe epilepsy. J Neurosci Methods. 2008;172:143-57.

34. Lemos T, Cavalheiro EA. Suppression of pilocarpine-induced status epilepticus and the late development of epilepsy in rats. Exp Brain Res. 1995;102:423-8.

35. Russmann V, Brendel M, Mille E, Helm-Vicidomini A, Beck R, Günther L, et al. Identification of brain regions predicting epilep- togenesis by serial [(18)F]GE-180 positron emission tomography imaging of

Published in : Epilepsia. 2019;60:2325-2333.
DOI: DOI: 10.1111/epi.16353
Status : Postprint (Author's version)

neuroinflammation in a rat model of temporal lobe epilepsy. Neuroimage Clin. 2017;15:35-44.

36. Vezzani A, Friedman A, Dingledine RJ. The role of inflammation in epileptogenesis. Neuropharmacology. 2013;69:16-24.

37. Rana A, Musto AE. The role of inflammation in the development of epilepsy. J Neuroinflammation. 2018;15:144.

38. Bergstrom M, Kumlien E, Lilja A, Tyrefors N, Westerberg G, Langstrom B. Temporal lobe epilepsy visualized with PET with 11C-L-deuterium-deprenyl-analysis of kinetic data. Acta Neurol Scand. 1998;98:224-31.

39. Kumlien E, Nilsson A, Hagberg G, Langstrom B, Bergstrom M. PET with 11C-deuterium-deprenyl and 18F-FDG in focal epilepsy. Acta Neurol Scand. 2001;103:360-6.

40. Venneti S, Lopresti BJ, Wiley CA. Molecular imaging of microg- lia/macrophages in the brain. Glia. 2013;61:10-23.

41. Mirzaei N, Tang SP, Ashworth S, Coello C, Plisson C, Passchier J, et al. In vivo imaging of microglial activation by positron emission tomography with [(11)C]PBR28 in the 5XFAD model of Alzheimer's disease. Glia. 2016;64:993-1006.

42. Thackeray JT, Hupe HC, Wang Y, Bankstahl JP, Berding G, Ross TL, et al. Myocardial inflammation predicts remodeling and neuroinflammation after myocardial infarction. J Am Coll Cardiol. 2018;71:263-75.

43. Rattka M, Brandt C, Bankstahl M, Broer S, Loscher W. Enhanced susceptibility to the GABA antagonist pentylenetetrazole during the latent period following a pilocarpine-induced status epilepticus in rats. Neuropharmacology. 2011;60:505-12.